

Article

A New Methodology for Determination of Layered Injection Allocation in Highly Deviated Wells Drilled in Low-Permeability Reservoirs

Mao Li ^{1,2,*}, Zhan Qu ^{1,2}, Songfeng Ji ³, Lei Bai ⁴ and Shasha Yang ⁵¹ School of Petroleum Engineering, Xi'an Shiyou University, Xi'an 710065, China; zhqu@xsyu.edu.cn² The Key Laboratory of Well Stability and Fluid & Rock Mechanics in Oil and Gas Reservoir of Shaanxi Province, Xi'an Shiyou University, Xi'an 710065, China³ Exploration and Development Research Institute, Changqing Oilfield Company, PetroChina, Xi'an 710018, China; jsf11_cq@petrochina.com.cn⁴ No.1 Oil Production Plant, Changqing Oilfield Company, PetroChina, Yan'an 716000, China; bailei612_cq@petrochina.com.cn⁵ School of Petroleum Engineering and Environmental Engineering, Yan'an University, Yan'an 716000, China; sarayang@yau.edu.cn

* Correspondence: 19111010004@stumail.xsyu.edu.cn

Abstract: During the water injection development process of highly deviated wells in low-permeability reservoirs, the water flooding distance between different layers of the same oil and water well is different due to the deviation of the well. In addition, the heterogeneity of low-permeability reservoirs is strong, and the water absorption capacity between layers is very different. This results in poor effectiveness of commonly used layered injection methods. Some highly deviated wells have premature water breakthroughs after layered water injection, which affects the development effect of the water flooding reservoirs. Therefore, based on the analysis and research of the existing layered injection allocation method and sand body connectivity evaluation method, considering the influence of sand body connectivity, the real displacement distance of highly deviated wells, reservoir physical properties, and other factors, a new methodology for determination of layered injection allocation in highly deviated wells drilled in low-permeability reservoirs is proposed. In this method, the vertical superposition and lateral contact relationship of a single sand body are determined using three methods: sand body configuration identification, seepage unit identification, and single sand body boundary identification. The connectivity coefficient, transition coefficient, and connectivity degree coefficient are introduced to quantitatively evaluate the connectivity of sand bodies and judge the connectivity relationship between single sand bodies. The correlation formula is obtained using the linear regression of the fracture length and ground fluid volume, and the real displacement distance of each layer in highly deviated wells is obtained. The calculation formula of the layered injection allocation is established by analyzing the important factors affecting the layered injection allocation, and a reasonable layered injection allocation is obtained. The calculation parameters of this method are fully considered, the required parameters are easy to obtain, and the practicability is strong. It can provide a method reference for the policy adjustment of layered water injection technology in similar water injection development reservoirs.

Keywords: highly deviated well; layered injection allocation; sand body connectivity; single sand body; flow unit; low-permeability reservoir; Ordos Basin; Huaqing area



Citation: Li, M.; Qu, Z.; Ji, S.; Bai, L.; Yang, S. A New Methodology for Determination of Layered Injection Allocation in Highly Deviated Wells Drilled in Low-Permeability Reservoirs. *Energies* **2023**, *16*, 7764. <https://doi.org/10.3390/en16237764>

Academic Editor: Pål Østebø Andersen

Received: 25 October 2023
Revised: 17 November 2023
Accepted: 22 November 2023
Published: 24 November 2023



Copyright: © 2023 by the authors. Licensee MDPI, Basel, Switzerland. This article is an open access article distributed under the terms and conditions of the Creative Commons Attribution (CC BY) license (<https://creativecommons.org/licenses/by/4.0/>).

1. Introduction

In the process of water injection development in low-permeability reservoirs, the water absorption capacity of different reservoirs is different due to the heterogeneity of reservoirs. During general water injection, most of the injected water is absorbed by the high-permeability reservoir, resulting in uneven water absorption in each reservoir, a

low degree of utilization in some reservoirs, and a low utilization rate of water injection. With the extension of water injection time, reservoir heterogeneity becomes more serious, and a fingering flow is formed in high-permeability reservoirs (Figure 1), resulting in premature water breakthrough and low ultimate recovery. In order to improve the current situation of reservoir water injection development, a layered water injection technology is proposed. This technology uses a packer to combine layers with similar reservoir physical properties and development conditions into one layer for water injection. The nozzle of the water distributor limits the water injection volume of the layer with a good development effect, improves the water injection volume of the layer with low-permeability or poor development effect, and improves the uneven distribution of injected water in the vertical direction [1]. Through layered water injection, high-permeability reservoirs do not form a single-layer breakthrough, while low-permeability or poor development effect in a reservoir improves the efficiency of water flooding, to alleviate inter-layer interference, increase the swept volume of water flooding, improve the effect of water injection development, and achieve the purpose of long-term high and stable production and enhanced oil recovery.

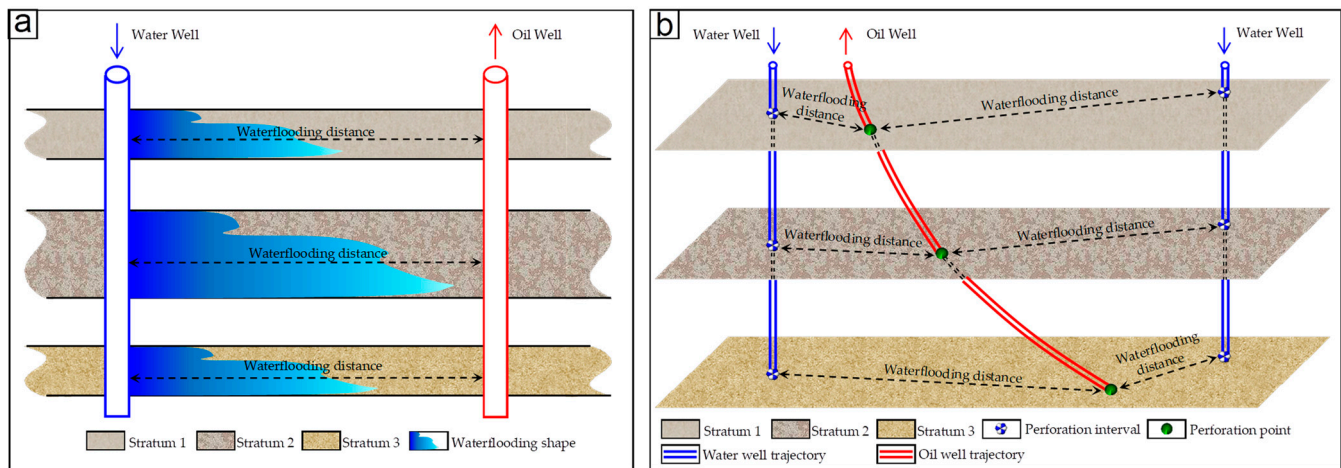


Figure 1. Displacement distance of water injection development in vertical wells (a) and highly deviated wells (b).

In the water injection development reservoir, in the case of the injection–production balance in the well group, the water injection volume is basically equal to the liquid production by the corresponding oil well. Therefore, the layered water injection volume of the corresponding water injection well can be quantitatively calculated using the layered liquid production of the oil well [2].

According to the basic formula of oil well production,

$$Q = \frac{2\pi kh\Delta P}{\mu_o \left(\frac{\ln r_e}{r_w} + S \right)}, \quad (1)$$

The production of oil wells is related to geological conditions (such as effective thickness (h), permeability (k), and crude oil viscosity (μ_o)) and development conditions (such as well spacing radius (r_e), wellbore radius (r_w), production pressure difference (ΔP), and transformation measures (S)). Effective thickness represents the thickness of the connected sand body, and the well spacing radius represents half of the distance between oil and water wells. In the calculation of layered injection allocation, these factors should be considered comprehensively to divide the water injection volume reasonably.

The key to layered water injection is to determine a reasonable layered injection allocation. Research methods of previous scholars' reasonable layered injection allocation are categorized and analyzed, including 18 different methods [3–15] (Table 1). According to the number of parameters and analysis methods, the methods are divided into single parameter

methods [3,4], multiparameter methods [3–10], and mathematical model methods [11–15]. According to geological and development conditions, the methods are divided into geological factors [3–5], development factors [3,4,6,11–14], comprehensive factors [2,7–10], and economic factors [15], among which the comprehensive factors consider geological factors and development factors. The single parameter method is commonly used in the early stage of layered water injection research. Due to the single consideration, the effect is not ideal. In recent years, the multiparameter method and mathematical model method have been gradually formed, but these methods have certain limitations. Most of them have difficulty in obtaining or quantifying parameters and do not consider the connectivity of sand bodies, so they cannot be applied to reservoir water injection development and production.

Table 1. Determination method of the reasonable layered injection allocation and its limitations.

Parametric Classification	Factor Classification	Method Classification	Method Characteristics	Limitations
Single parameter	Geological factors	Effective thickness method [3]	The layered injection allocation is determined with the ratio of the oil-producing section to the total oil-producing section.	This method considers incomplete parameters.
		Connected thickness method [4]	The layered injection allocation is determined with the ratio of the connected thickness of the sand body to the thickness of the oil well.	
	Development factors	Injection–production ratio method [3]	The layered injection allocation is ascertained by dividing the injection production ratio of each individual layer by the total injection production ratio.	The injection–production ratio of each layer is difficult to obtain.
		Liquid production intensity method [4]	The layered injection allocation is quantitatively analyzed through the multiplication of three factors: the perforation thickness, the connectivity coefficient, and the intensity of water injection in each layer.	The connectivity coefficient and water injection intensity data of each layer are difficult to obtain.
Multiparameter	Geological factors	Stratigraphic coefficient method [3]	Using the weighted formation coefficient, the water injection splitting coefficient of each layer is obtained.	This method considers incomplete parameters.
		Sand body connectivity evaluation Stratigraphic coefficient method [5]	The sand body connectivity is divided into three categories by sedimentary facies, and the water injection is divided by combining the physical parameters.	The reason for sand body connectivity is not sufficient.
		Remaining oil distribution method [6]	The layered injection allocation is obtained using the quantitative relationship between the recovery degree and the cumulative injection pore volume multiples.	The water absorption data acquisition is difficult.
	Comprehensive factors	Revised coefficient method [4]	Considering the injection–production balance, water cut rise rate, pump efficiency, and other factors, the empirical formula is obtained.	1. This method considers many parameters and it is difficult to obtain some data. 2. There are many artificial coefficients, which easily cause errors.
		Splitting coefficient method [2]	According to geological conditions, oil displacement conditions, and mining conditions of the reservoir, the water injection volume is allocated according to the weight of the relevant parameters.	
		Balanced displacement method	Considering the physical properties and utilization status of each layer, the layered injection allocation relationship is established [7].	1. It is difficult to obtain layered recovery degree data. 2. The connectivity of sand bodies in each layer is not considered.

Table 1. Cont.

Parametric Classification	Factor Classification	Method Classification	Method Characteristics	Limitations
Mathematical model	Comprehensive factors	Balanced displacement method	The layered injection allocation is obtained using the quantitative relationship between the recovery degree and the injection pore volume multiples [8].	1. This method requires a lot of experimental support, which cannot be replicated. 2. The connectivity of sand bodies in each layer is not considered.
		Seepage resistance coefficient method [10]	The layered injection allocation is obtained using the idea of displacement flux equalization [9]. The vertical splitting coefficient of water injection well is determined using seepage resistance coefficient.	This method does not consider the connectivity of sand bodies in each layer.
	Development factors	Multiple regression method [11]	A multiple sequence regression model is formulated, drawing from the dynamic production data of both the central water injection well and the surrounding production wells within the well group.	These methods are aimed at the optimization of well group injection allocation and cannot realize the optimization of layered injection allocation.
		Neural network method [12]	The relationship model between liquid production and water injection is established using neural network technology.	
		Conductivity method [13]	The connectivity of the unit is characterized by its electrical conductivity and connected volume.	
Economic factors	Capacitance–resistance method [14]	The formula for estimating water flooding in layered reservoirs is derived from the capacitance–resistance model equation.	This method considers many parameters, and it is difficult to obtain oil production and water injection of each layer.	
	Net present value method [15]	The water injection cycle, injection volume, and production should be adjusted based on the maximum net present value of production.	This method from the economic evaluation does not consider formation and development factors.	

Conventional vertical well development is generally single-layer development. The development of reservoirs in highly deviated wells can achieve the multilayer development of one well, maximize the reservoir drainage area, improve the single-well productivity and ultimate recovery, and reduce the number of drilling wells and development costs [16–19]. It is widely used to increase and stabilize production in old oilfields, offshore oilfields, and low-permeability oilfields.

In conventional vertical well water injection development, oil and water wells are all vertical wells, and the displacement distance between the connected sand bodies is the distance between the oil and water wells (Figure 1a). However, in water injection development of highly deviated wells, due to the different perforation points of different layers, the water flooding distance between the same water injection well and different layers of highly deviated wells is different, and the water flooding distance between different water injection wells and the same layer of highly deviated wells is also different (Figure 1b), which makes it difficult to determine the reasonable layered water injection policy. Unreasonable layered water injection can easily lead to premature water breakthroughs in highly deviated wells, reduce the final recovery rate, and affect the development effect of the reservoir.

Scholars' research on highly deviated wells mostly focuses on drilling [20], logging [21–24], fracturing [25,26], productivity evaluation [27,28], seepage law research [29–31], etc. However, no relevant reports on the study of reasonable layered injection allocation in highly deviated wells have been found.

Through the influencing factors of layered injection allocation, it can be known that permeability, crude oil viscosity, wellbore radius, production pressure difference, and transformation parameters are easy to obtain, but sand body connectivity data need to be determined after the evaluation of sand body connectivity, and the water drive distance between different layers of highly deviated wells needs to be calculated. Therefore, a new methodology for determination of layered injection allocation in highly deviated wells drilled in low-permeability reservoirs is established. This method is based on the evaluation of sand body connectivity and clarifies the connectivity and water flooding distance of each sand body between highly deviated wells and water injection wells, to reasonably split the layered water injection volume of water injection wells.

2. Geological Background

Water injection development of highly deviated wells in low-permeability reservoirs in China is mainly concentrated in the Yanchang Formation reservoir in the Ordos Basin. Notably, the highly deviated wells water injection development of low-permeability reservoirs in the Huaqing area of the Ordos Basin has been scaled up, and the well network is perfect. Therefore, the Ordos Basin's Huaqing area serves as a model for similar developments in the basin, so the Chang 6₃ reservoir in the Huaqing area is selected as the target area for research.

The Ordos Basin is a large oil- and gas-bearing basin in central China. It separated from the North China Plate in the Late Triassic and has evolved independently to this day. It belongs to a multicycle cratonic basin [32] and is currently constructed as a gentle westward dipping monocline with a slope of less than 1° [33]. Based on the history of the basin's structural evolution and current structural development characteristics, the Ordos Basin is divided into six primary structural units (Figure 2a): Yimeng Uplift, Western Edge Thrust Belt, Tianhuan Depression, Yishan Slope, Western Shanxi Folding Belt, and Weibei Uplift [34]. The Mesozoic oil resources in the Ordos Basin are vast, with the Triassic Yanchang Formation being one of the main exploration and development target layers in the basin. It belongs to lacustrine basin sedimentation, deltaic sedimentation, and deep-water gravity flow sedimentation, which are widely developed [35,36]. The Yanchang Formation is divided into 10 oil layers from Chang 10 to Chang 1, from bottom to top [37], which has experienced a complete sedimentary cycle of river–delta–lake–delta–river.

Huaqing area is located in the southwest of Yishan Slope (Figure 2a). The research target interval is the Chang 6₃ oil layer group, with an average formation thickness of 45 m. The sedimentary system is turbidite sedimentation, which belongs to a type of deep-water gravity flow sedimentary system. It is further divided into turbidite channel, side-turbidite channel, and inter-turbidite channel microfacies. The turbidite channel and side-turbidite channel microfacies constitute the sand body sedimentary skeleton, which is the main oil and gas reservoir (Figure 2b). The average permeability of the Chang 6₃ reservoir group is 0.28 mD, which indicates a typical low-permeability lithologic reservoir.

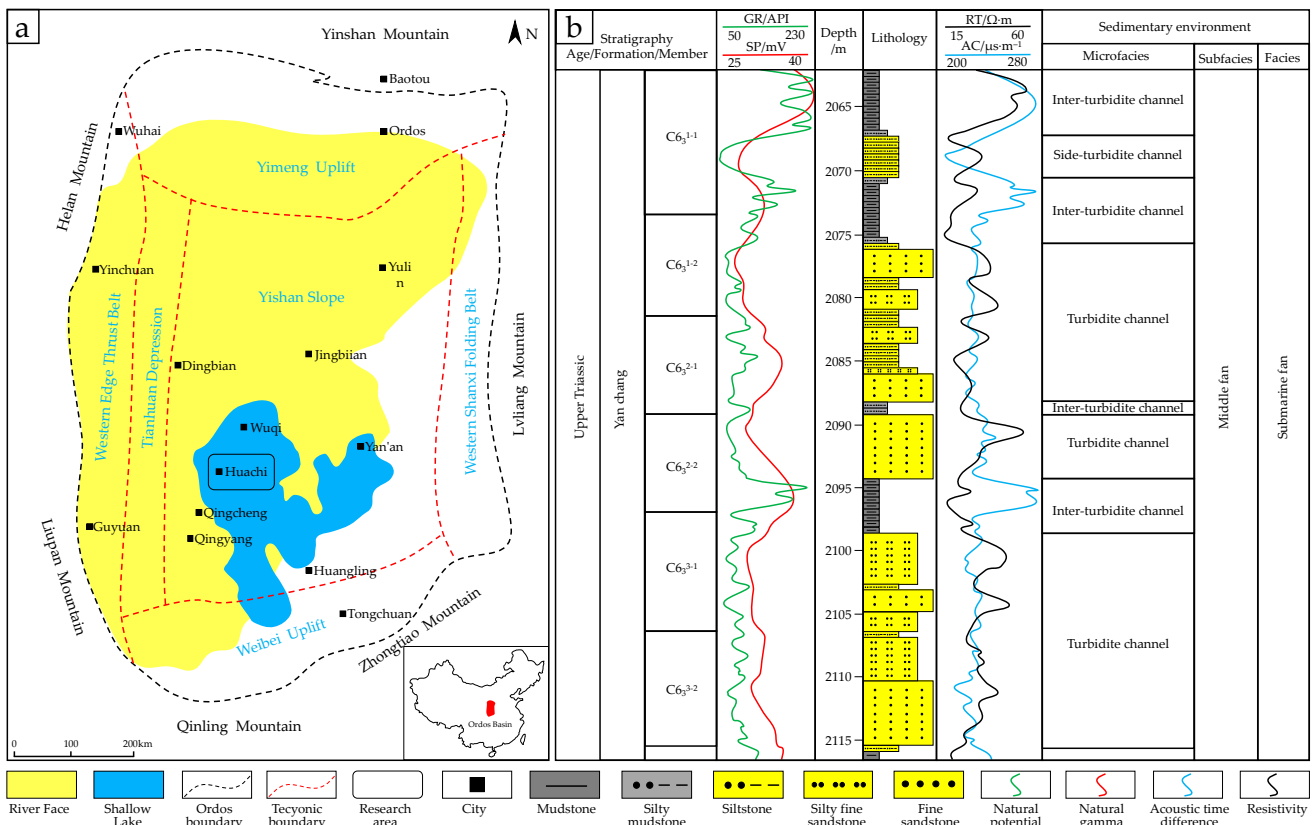


Figure 2. Ordos Basin tectonic unit and Yanchang Formation comprehensive histogram. (a) Ordos Basin structure and the location of the study area. (b) Comprehensive histogram of the Chang 6₃ oil-bearing formation in the Huaqing area, Ordos Basin. In the figure, SP, GR, RT, and AC represent natural potential, natural gamma, resistivity and acoustic time difference, respectively.

3. Sand Body Connectivity Evaluation

The evaluation of reservoir connectivity is divided into three types: inter-sand body connectivity, sand body and well connectivity, and inter-well connectivity. The connectivity between sand bodies can be described as the ratio of the volume of connected sand bodies to the total volume or as the average contact percentage of sand bodies. Sand body and well connectivity is the ratio of the volume of the drilled reservoir to the total volume of the reservoir. Inter-well connectivity can be defined as the proportion of sand bodies drilled by two adjacent wells in the whole reservoir [38]. Scholars mostly focus on inter-well connectivity and inter-sand body connectivity in reservoir connectivity evaluation [39,40], and inter-well connectivity [41–44] is mostly studied by means of dynamic monitoring data. The connectivity between sand bodies is mostly studied by outcrop [41], seism [42], sedimentary characteristics [43], and sand body configuration [44], but there are limitations. Inter-well connectivity relies too much on dynamic monitoring data, and it is impossible to judge inter-well connectivity without dynamic monitoring data. There are various methods for evaluating the connectivity between sand bodies, but none of them can clarify the connectivity between different sand bodies (Table 2).

The connectivity evaluation of a water injection development reservoir refers to the analysis of sand body connectivity. Judging the vertical and lateral connectivity of sand bodies is the premise of studying sand body connectivity. In the absence of dynamic monitoring data and seismic data, it is necessary to clarify the connectivity between each sand body.

Table 2. Reservoir connectivity evaluation method and its limitations.

Evaluation Type	Evaluation Method	Method Characteristics	Limitations
Inter-well connectivity	Dynamic monitoring method	The connectivity between oil and water wells is judged using dynamic monitoring data [39,40].	This method cannot judge the inter-well connectivity without dynamic monitoring data or seismic data interpretation.
	Seismic method	Based on seismic data, the connectivity of the sand body is analyzed [41].	
inter-sand body connectivity	Sand–ground ratio method	The connectivity of sand body is judged using the sedimentary structure model of sand body described by outcrop [42].	1. The accuracy of this method is low; 2. The method cannot effectively identify the sedimentary interface; 3. The method cannot clarify the connectivity between different sand bodies.
	Sandstone amalgamation method	Through the identification of sand mud facies, the degree of sandstone amalgamation is described. The higher the amalgamation rate, the better the connectivity [43].	
	Sand body configuration method	By analyzing the contact relationship of sand bodies, the connectivity of sand bodies is determined [44].	

The core of sand body connectivity evaluation is how to evaluate the connectivity and connectivity degree of sand bodies. Previous scholars only studied the connectivity relationship, and the research on the connectivity relationship was mostly in the stage of sedimentary interface and sand body configuration identification, without considering the seepage characteristics of sand bodies, resulting in low accuracy of sand body connectivity identification. Notably, research on the connectivity degree of sand bodies has not been reported, but the connectivity degree of a sand body is the key to judge the connectivity of sand bodies. Therefore, a single sand body is introduced, and the connectivity evaluation between sand bodies is realized by combining sand body configuration identification, flow unit division, and sand body connectivity quantitative analysis. Sand body configuration reflects the geological sedimentary period and the evolution process of the basin. It is the spatial distribution direction, size, and mutual superposition relationship of each configuration unit. The flow unit is based on the reservoir lithology, physical properties, sedimentation, pore throat, and fluid characteristics to divide the reservoir into different seepage units, mainly reflecting seepage characteristics. Although sand body configuration identification [45–47] and flow unit division [48,49] have been studied by predecessors, how to combine the two methods to correct sand body connectivity has not been reported. After the combination of the two methods, boundary identification of single sand bodies is carried out, which corrects the deficiency of a single sand body identification with the sand body configuration and realizes an accurate evaluation of connectivity between sand bodies.

The specific implementation methods are as follows: (1) sand body configuration identification: identify the vertical stacking pattern and lateral contact relationship of sand bodies; (2) seepage unit identification: through the division of flow units, different seepage units are classified; (3) single sand body boundary identification: combined with the research results of (1) and (2), the quantitative prediction model of a single sand body is established using the width–thickness ratio of the sand body, and the identification results of (1) and (2) single sand body are corrected. Through comprehensive analysis and mutual correction of the above three steps, the connectivity between different reservoir sand bodies can be determined.

3.1. Identification of a Single Sand Body

A single sand body is defined as a geological unit that is continuous in the vertical and horizontal directions but separated from the upper and lower sand bodies by mudstone or impermeable interlayers [50]. Single sand body identification mainly studies its spatial distribution scale and superposition relationship.

3.1.1. Vertical Interface Characteristics and Stacking Patterns of Single Sand Body

Different single sand bodies form different superposition patterns in the vertical direction due to the differences in sedimentary periods, sedimentary environments, and sedimentary processes. Through the lithology electrical calibration in coring wells and the analysis of sand body configuration using high-resolution sequence stratigraphy, it is found that the logging curves of different single sand bodies have completely different amplitude and morphological characteristics, and the vertical stacking patterns of four types of single sand bodies in Chang 6₃ oil layer group are summarized (Figure 3).

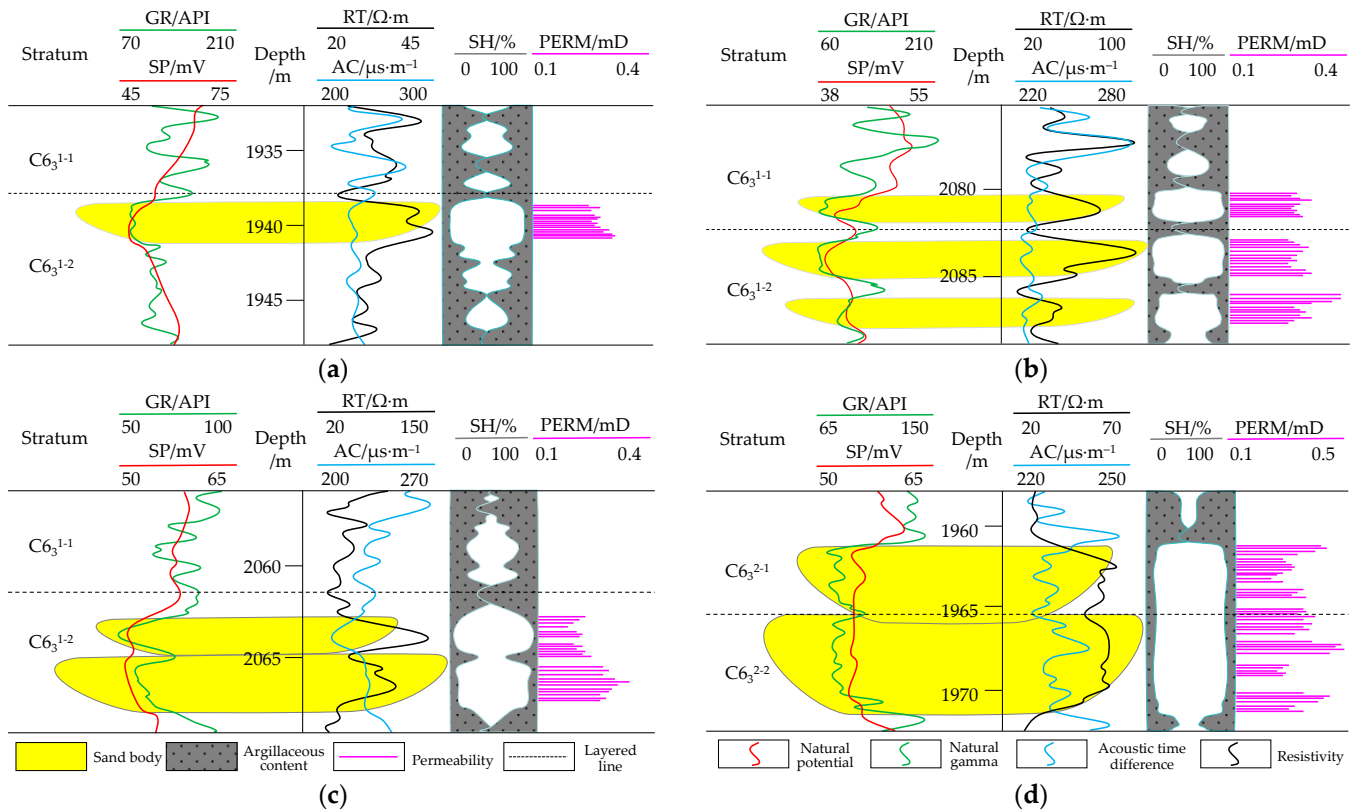


Figure 3. Vertical stacking pattern and logging curve identification of the Chang 6₃ reservoir group in the Huaqing area. In the figure, SH and PERM represent argillaceous content and permeability. (a) Isolated vertical interface characteristics of the L419-9 well, (b) separated vertical interface characteristics of the B185-117 well, (c) superimposed vertical interface characteristics of the B179-113 well, (d) cut and stacked vertical interface characteristics of the B185-109 well.

(1) Single-period channel vertical isolated type

This kind of sand body is formed by single-period turbidite channel sand body sedimentation. The core physical property experiments show that the permeability at the bottom of the sand layer is the highest, and the physical property at the top is poor, showing the characteristics of positive rhythm. The logging curve of this kind of single sand body shows that the gamma ray is mostly box-shaped, and the top and bottom reenter obviously, which is close to the mudstone baseline; the natural potential and resistivity are mostly high-amplitude box- or bell-shaped. The sand body is separated by a thick argillaceous

interlayer, and no other sand bodies appear in the layer (Figure 3a). Due to the development of sand bodies in the Chang 6₃ oil layer group, there are few vertical isolated single sand bodies, which are mainly distributed in the inter-turbidite channels microfacies, with a frequency of 8%.

(2) Multiperiod channel vertical separation type

The turbidite channel sand body of the next period is gradually developed, and the argillaceous sediments of the previous period are continuously eroded, but it has not yet eroded to the top of the sedimentary sand body. At this time, there is a stable argillaceous interlayer distribution between the sand bodies. The argillaceous content of the interlayer is more than 50%, and the argillaceous content mirror curve intersects (Figure 3b). The logging curve of this kind of single sand body shows obvious reentrant characteristics of gamma ray and resistivity. The vertical separated single sand body is mainly distributed in the side-turbidite channel microfacies, with a frequency of 18%.

(3) Multiperiod channel vertical superposition type

Due to the difference between the sedimentation rate and the sediment recharge rate, the spatial position relationship of the turbidite channel sand body changes. If the sand body formed in the next period is strong enough to erode the sand body of the previous period, the mudstone or impermeable interlayer between the two sand bodies is completely washed away, and the next sand body is finally placed on top of the sand body of the previous period. The physical properties between the next period and the previous sand bodies become worse, and fine-grained sediments are developed. The argillaceous content of the sand body increases and is generally 10–30%. The mirror curve of the shale content does not intersect (Figure 3c). The superposition relationship of single sand bodies can be quickly judged using the characteristics of the mirror curve of the argillaceous content. The logging curve of this kind of single sand body shows reentrant characteristics of gamma ray and resistivity, but the reentrant amplitude is less than that of the vertical separation. The vertical superimposed single sand body is mainly distributed in the turbidite channel microfacies, with a frequency of 26%.

(4) Multiperiod channel cutting and stacking type

Due to the erosion and vertical erosion of the channel in the next period, the fine-grained sedimentary sand bodies in the upper part of the channel in the previous period are eroded, transported, and deposited, so that the coarse-grained material of the channel in the previous period is directly in contact with the retention deposits at the bottom of the channel in the next period. The sand bodies in the two periods are obviously cut and stacked, the physical properties are similar, and the argillaceous content is almost unchanged (Figure 3d). The logging curve of this kind of single sand body shows slight reentrant characteristics of gamma ray and resistivity. Due to the fast sedimentation rate and sediment supply rate of the turbidite sedimentary system, the channel sand bodies in the previous period are mostly cut by the next period. The multiperiod channel cutting and stacking type is the most developed, mainly distributed in the turbidite channel microfacies, with a frequency of 48%.

3.1.2. Lateral Contact Relationship and Identification Mark of a Single Sand Body

Lateral contact is the positional relationship of different single sand bodies on the plane. Generally, the top surface of the sedimentary sand body in the same period has a similar height. Sedimentary sand bodies in different periods often form terraces with obvious elevation differences due to different erosion times, and the lateral contact of different single sand bodies will form different cutting patterns. On the basis of the single well identification of each genetic sand body type, five types of lateral contact patterns of the single sand body in the Chang 6₃ oil layer group are summarized.

(1) Inter-bay contact

Inter-bay contact means that the two adjacent sand bodies are separated by the inter-turbidite channel and do not contact directly, which indicates the termination of lateral erosion of the turbidite channel. The two sand bodies are filled with muddy sediments, so they are not connected, and each has an independent seepage system. The inter-turbidite channels' logging curve shows a low amplitude and relatively flat state, and the physical properties are poor. It cannot be used as a channel for oil and gas seepage and can be used as a basis for single sand body identification (Figure 4a).

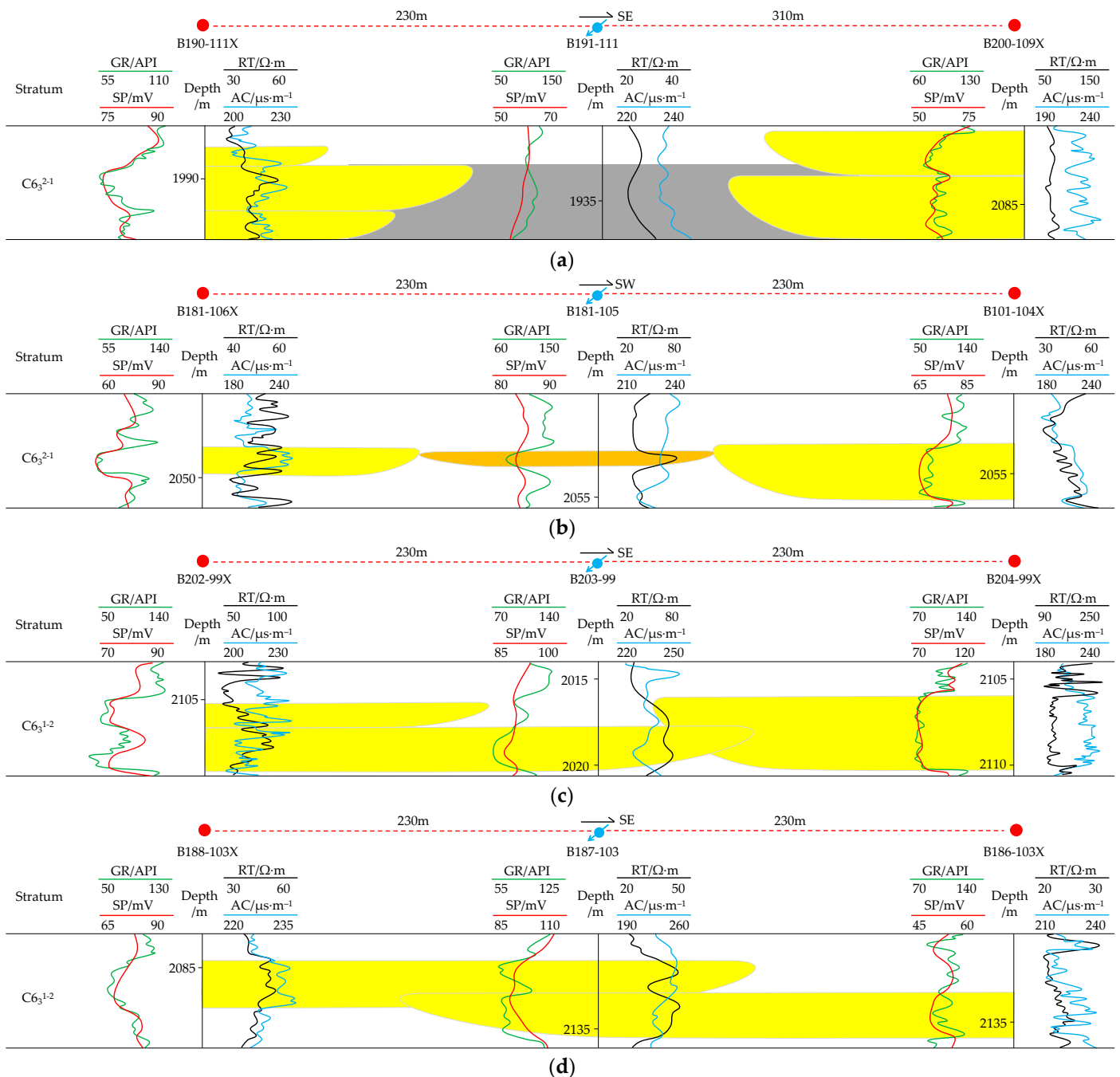


Figure 4. Cont.

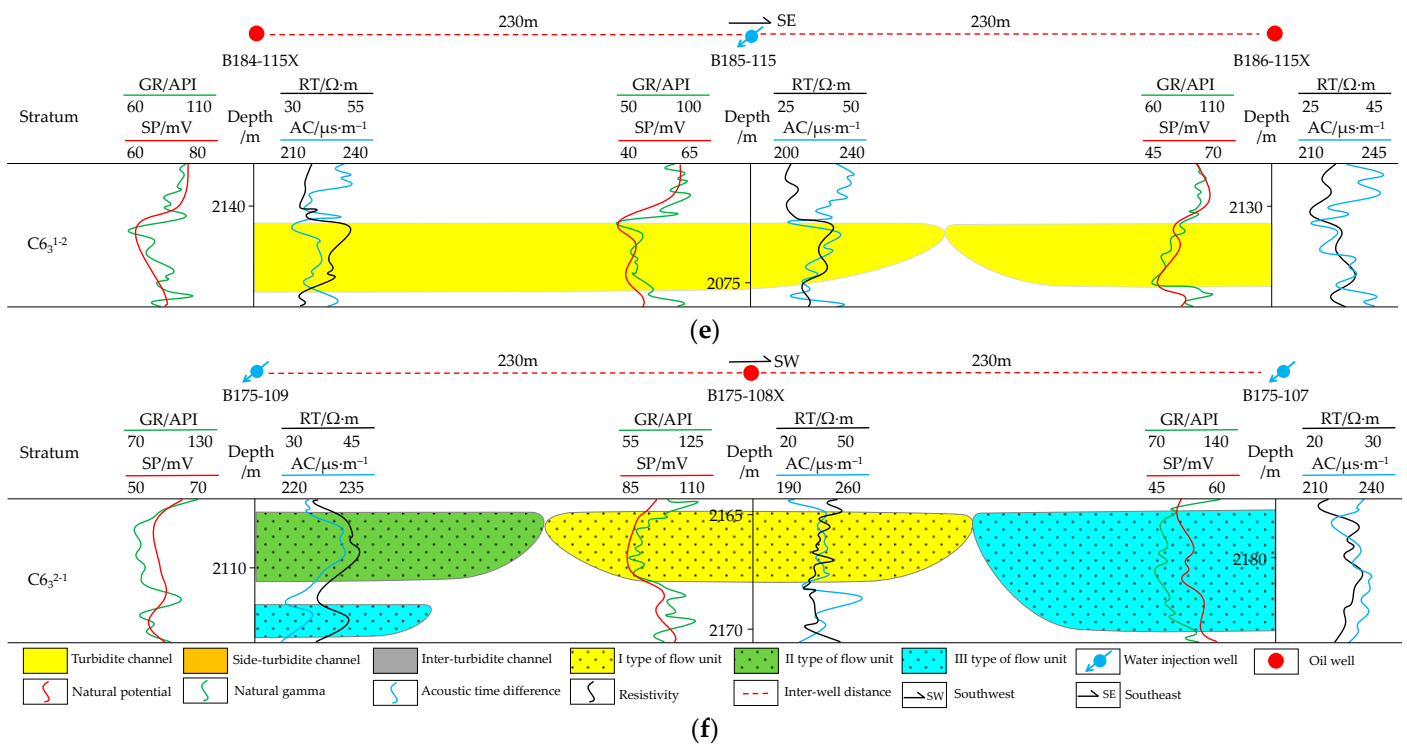


Figure 4. Lateral contact pattern and logging curve identification of the Chang 6_3 reservoir group in the Huaqing area. (a) Inter-bay contact, (b) levee contact, (c) side-cut contact, (d) substitutive contact, (e) class I docking contact, (f) class II docking contact.

(2) Levee contact

Levee contact refers to gradual thinning of the thickness of the middle connection between two periods of sand bodies and the deterioration of physical properties, reflecting the process of sedimentary microfacies' change, marking the emergence of the sedimentary boundary of the single-period turbidite channel, which can be used as the basis for single sand body identification. The two sand bodies are connected by sand bodies similar to levees, and the connectivity is weak or discontinuous, meaning that they cannot be used as a channel for oil and gas seepage. The gamma ray and resistivity curves of the levee sand body are finger-shaped (Figure 4b).

(3) Side-cut contact

Due to the migration of the mainstream line of the channel, the sedimentary channels in different periods often have characteristics of cutting and filling each other, resulting in lateral superposition of the sedimentary channels in the two periods, marking the development of the channels in different periods, which can be used as an identification mark of a single sand body. There is a large amount of contact between the two sand bodies, indicating that they have good connectivity and can be used as a channel for oil and gas seepage. Because it is a different sand body, the logging curve shape is different (Figure 4c).

(4) Substitutive contact

There is an elevation difference between the two sand bodies. Strong erosion and undercutting of the channel in the next period make the sand body partially eroded in the previous period, and the complete shape cannot be retained. The two periods' channel sand bodies are vertically cut and stacked into a false continuous shape, and even the phenomenon of mutual substitution between sand bodies occurs. In the two periods of sand body cutting and folding parts, the gamma ray and resistivity curves are obviously reentrant (Figure 4d). The two sand bodies are in contact with each other and generally have good connectivity, meaning that they can be used as a channel for oil and gas seepage.

(5) Docking contact

The elevation and thickness of the two sand bodies are basically the same, but the logging curve shape is obviously different, which shows that the lithofacies combination and sedimentary rhythm of different sand bodies are significantly different, indicating that the sedimentary environment of the two sand bodies is different, which can be used as the identification mark of a single sand body. For example, the sand body of well B185-115 has reverse rhythm, and the sand body of well B186-115X has positive rhythm, which belong to different genetic types of sand bodies. The two sand bodies are almost not in contact with each other, and connectivity is weak or discontinuous, so they cannot be used as a channel for oil and gas seepage (Figure 4e).

There is another special case of docking contact. The elevation, thickness, and logging curve shape of the two sand bodies are similar. Through the analysis of sand body configuration, it is considered to be the same sand body. However, in the dynamic verification of water injection development, water injection is not effective, and the flow unit is not the same period sand body, which is the docking contact of the two sand bodies. For example, there is a single sand body boundary between well B175-109 and well B175-108X (Figure 4f).

3.2. Single Sand Body Division Method

3.2.1. Flow Unit Division of Single Sand Body

The concept of a flow unit is defined as the volume of the total reservoir rock within which the geological and petrophysical properties that affect the fluid flow are internally consistent and different from the properties of other rock volumes. Within each flow unit, the geological parameters affecting the fluid flow are similar, while the differences in lithology and rock physical properties are shown between each flow unit [48]. The flow unit is controlled by macro-sedimentation and microphysical properties, which are not always consistent with geological lithofacies. The reservoir can be divided into different types of reservoir rocks by flow unit [51].

The flow unit division parameters are divided into the following four types: the first is the parameters reflecting the macroscopic reservoir characteristics (porosity and permeability), the second is the parameters reflecting the sedimentary environment (effective thickness, median grain size, and argillaceous content), the third is the parameters reflecting the microscopic pore structure (pore throat radius and flow zone index [52]), and the fourth is the parameters reflecting the fluid characteristics (oil saturation, irreducible water saturation, viscosity, density, volume coefficient, etc.). Considering the difficulty of parameter acquisition and the coverage of parameters, five parameters are selected to carry out the flow unit division, among which are the porosity parameter, characterizing the reservoir storage capacity; the permeability parameter, characterizing the seepage capacity; the argillaceous content parameter, characterizing the sedimentary environment; the flow zone index parameter, characterizing the pore throat structure; and the oil saturation parameter, characterizing the fluid characteristics.

Using IBM SPSS statistics version 19 software, the five most representative parameters of 4790 sand bodies in Chang 6₃ reservoir are clustered and divided into three types. The discriminant coincidence rate is greater than 95%, which meets the accuracy requirements of cluster analysis. The results show that there are 2520 single sand bodies in the type I flow unit, 787 single sand bodies in the type II flow unit, and 1483 single sand bodies in the type III flow unit (Figure 5). Type I represents the strong reservoir seepage capacity of sand bodies, mainly located in turbidite channels, with weak heterogeneity and high oil saturation. Type II represents the slightly poor reservoir seepage capacity of sand bodies, mainly located on the side-turbidite channels, with medium heterogeneity and oil saturation. Type III represents the worst reservoir seepage capacity of sand bodies, mainly located in inter-turbidite channels, with strong heterogeneity and the lowest oil saturation.

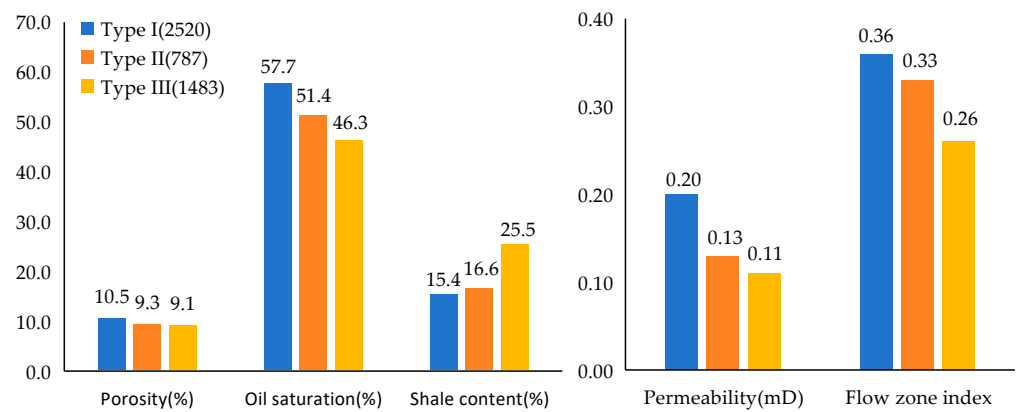


Figure 5. Flow unit division of the Chang 6₃ reservoir in the Huaqing area.

3.2.2. Quantitative Prediction of a Single Sand Body Boundary

Based on the results of sand body configuration and flow unit division, by counting the width and thickness data of different sedimentary microfacies sand bodies in the Chang 6₃ reservoir, it is determined that the width–thickness ratio of the single sand body of the turbidite channel microfacies is 50~120, and the width–thickness ratio of the single sand body of the side-turbidite channel microfacies is 70~120. The empirical formula of the width–thickness ratio of a single sand body is obtained using multiple regression (Figure 6): the turbidite channel is $W = 239.97e^{0.097h}$, and the side-turbidite channel is $W = 141.52e^{0.248h}$. Under the condition that the thickness of a single sand body is known, the empirical formula can be used to clarify the extension width of a single sand body in different sedimentary microfacies and to correct the sand body configuration and flow unit division results.

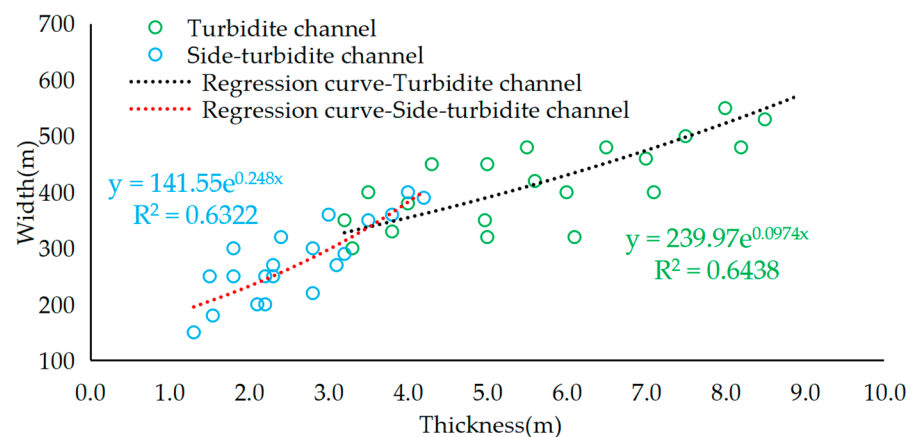


Figure 6. Regression curve of the width–thickness ratio of a turbidite channel and a single sand body on the side-turbidite channel of the Chang 6₃ oil layer in the Huaqing area.

3.2.3. Example of the Flow Unit Correction and Single Sand Body Contact Relationship

Under the identification of sand body configuration, the logging curve shape, top elevation, and thickness of the No.2 and No.3 sand bodies of Well A and Well B are similar, and they are considered to be the same sand body and can be directly connected (Figure 7a). With the verification of flow units, it can be seen that the sand bodies of No.2 and No.3 in the two wells are different flow units, and the sand bodies are laterally cut and stacked. Due to the existence of seepage barriers, it can be seen from logging interpretation that No.2 and No.3 in Well A are water layers, and the No.2 and No.3 sand bodies in Well B are oil layers, which are different sedimentary sand bodies (Figure 7b). The flow unit is used to identify the single sand body configuration and improve the accuracy of single sand body division.

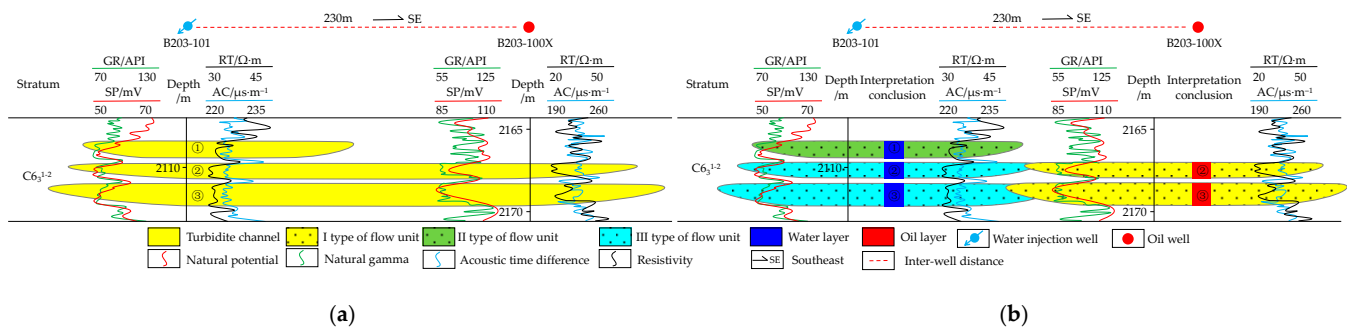


Figure 7. The flow unit corrects the contact relationship of a single sand body identified with sand body configuration. (a) Sand body configuration identification of the single sand body connectivity relationship. (b) Flow unit correction and single sand body connectivity relationship. In the figure, the circled numbers 1, 2, and 3 represent different sand body numbers.

3.3. Quantitative Evaluation of the Sand Body Connectivity

The quantitative evaluation of sand body connectivity is very important for water injection development reservoirs. Therefore, based on the identification results of sand body connectivity, three indexes of the connectivity coefficient (δ), transition coefficient (β), and connectivity degree coefficient (φ) are proposed to quantitatively evaluate sand body connectivity. The connectivity coefficient represents the connectivity ratio of the sand body, the transition coefficient represents the connectivity strength of the sand body, and the connectivity degree coefficient is the product of the connectivity coefficient and the transition coefficient, that is, $\varphi = \delta * \beta$, which represents the real connectivity of the sand body.

(1) Connectivity coefficient

The connectivity coefficient (δ) is the ratio of the thickness of the inter-well effectively connected sand body (H_c) to the total sand body thickness (H_t). The calculation formula is as follows:

$$H_c = \sum_{i=1}^n h_i, \quad (2)$$

$$\delta = H_c / H_t. \quad (3)$$

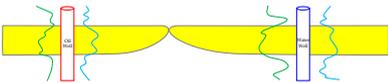
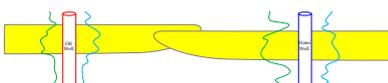
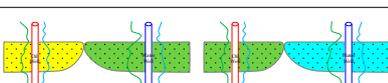
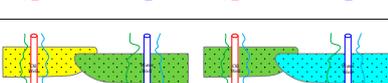
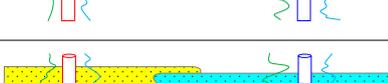
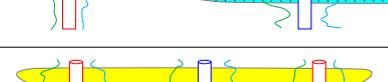
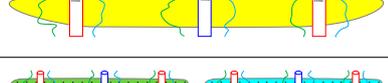
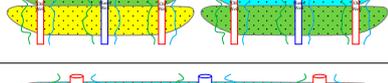
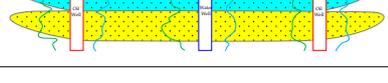
In the formula, n represents the number of connected single sand bodies, and h_i is the effective thickness of the i -th connected single sand body between single wells.

(2) Transition coefficient

The transition coefficient is the characterization of sand body connectivity under different single sand body contact relationships. There are differences in lithology, physical properties, heterogeneity, and seepage characteristics of different types of single sand bodies. There are seepage barriers between sand bodies under different contact relationships, and the strength of the connectivity is also different. According to the different single sand body contact modes and production performance verification results of several similar low-permeability reservoirs, the empirical values of transition coefficients under different contact modes are set, and the single sand body transition coefficients under different contact relations are classified and described from the vertical and lateral angles.

The lateral contact relationship of connected sand bodies is divided into seven types, and the transition coefficients are divided into six types, which are perfect, good, medium-good, medium, medium-poor, and poor, respectively. The corresponding transition coefficients are 1.0, 0.9, 0.8, 0.6, 0.4, and 0.2, respectively. The vertical superposition relationship of connected sand bodies is divided into three types, and the transition coefficients are also divided into three types, which are good, medium, and poor, respectively. The corresponding transition coefficients are 1.0, 0.6, and 0.4, respectively. With the identification of a single sand body, the contact relationship between connected sand bodies is evaluated, and the transition coefficient between sand bodies is determined (Table 3).

Table 3. Evaluation of single sand body connectivity.

Contact Type	Contact Relationship	Flow Unit Type	Elevation Difference (Yes/No)	Contact Mode	Connectivity	Transition Coefficient
Lateral	Connection (same sand body)	Same kind	No		Perfect	1.0
			Yes		Good	0.9
	Lateral cut type or substitution type (different sand body)	Same kind	No		Medium-good	0.8
			Yes		Medium	0.6
Lateral	Lateral cut type or substitution type (different sand body)	Class I and II or Class II and III	Yes		Medium-poor	0.4
		Class I and II or Class II and III	Yes		Medium-poor	0.4
		Class I and III	No		Poor	0.2
		Class I and III	Yes		Poor	0.2
Vertical	Cut and stack type	Same Kind			Good	1.0
		Class I and II or Class II and III			Medium	0.6
		Class I and III			Poor	0.4

Sand body

I type of flow unit

II type of flow unit

III type of flow unit

Natural gamma

Acoustic time difference

4. Calculation of Real Displacement Distance

The water injection development reservoir of highly deviated wells is a multilayer development. The displacement distance from the multilayer perforation position to the water injection well is different, but the displacement distance from the perforation position to the water injection well cannot represent the real displacement distance between oil and water wells. The real displacement distance refers to the shortest displacement distance between the fracture network of the same layer and the water injection well (Figure 8). In order to achieve reasonable layered water injection and improve the displacement effect, the real displacement distance between oil and water wells in different layers should be clarified first.

Taking B170-109 X as an example, the well was fractured in six sections, and the length, width, and height data of each fracture were obtained using microseismic monitoring (Figure 9, Table 4). Through the drawing of fracturing fractures, the real displacement distance between oil and water wells was measured with Geomap 3.6 software (Figure 8). Without considering the fracture network, the displacement distance from the injection well

B171-109 to the production well B170-109X is 350 m. Through the description of the fracture network, the real shortest displacement distance is 240 m. Through the stratigraphic profile of highly deviated wells and water injection wells, the real displacement distance between different layers of oil and water wells can be visually seen (Figure 10).

Table 4. Microseismic monitoring fracture data of B170-109x well.

Section	Fracture Length (m)			Fracture Width (m)	Fracture Height (m)	Fracture Strike (Northeast)
	West Flank	East Flank	Overall Length			
The first section	128	46	174	41	76	57°
The second section	159	131	290	62	49	61°
The third section	220	126	346	58	59	63°
The fourth section	267	134	401	60	60	66°
The fifth section	128	96	224	44	43	58°

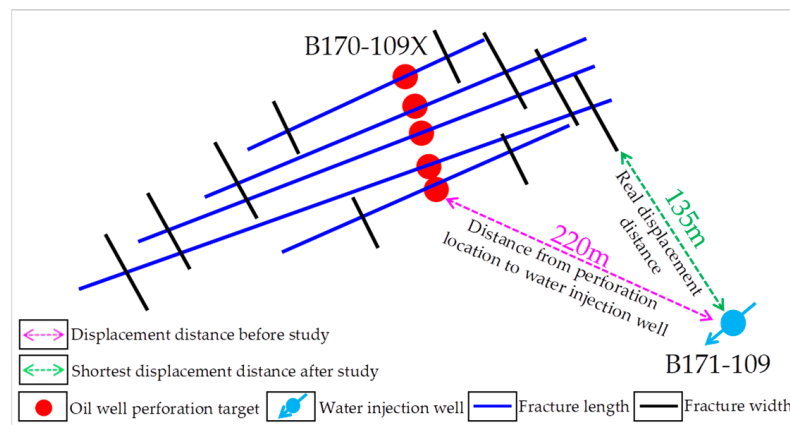


Figure 8. Plane position of the B170-109X well and the B171-109 well.

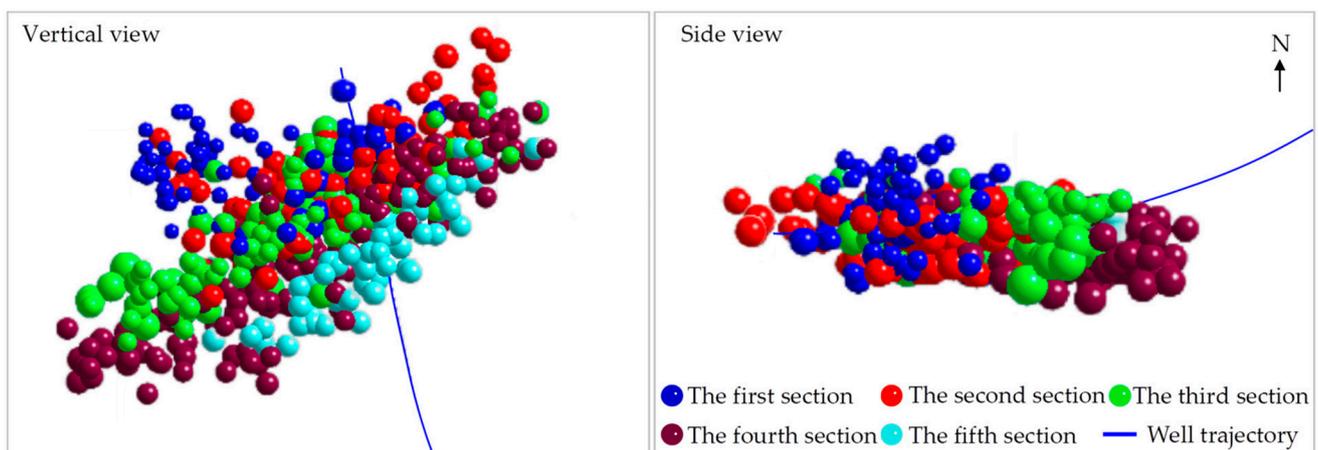


Figure 9. Microseismic monitoring results of the B170-109X well.

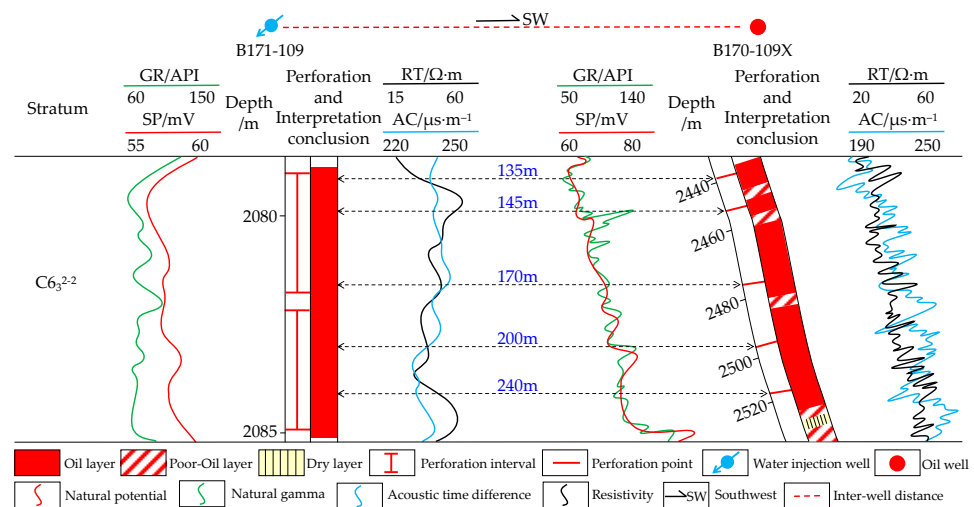


Figure 10. The B170-109X and B171-109 well stratigraphic profile (marked as the actual displacement distance).

Through statistical analysis of the microseismic monitoring data of low-permeability reservoirs in Ordos Basin, it is considered that there is a positive correlation between the ground fluid volume and the length of fracture [53]. Microseismic monitoring technology is the main means to describe fracture morphology, but its cost is high and it is difficult to achieve full coverage. Therefore, three to five typical wells under different fracturing scales can be selected for testing in water injection development reservoirs. Combined with the microseismic monitoring fracture data, the correlation formula is obtained using the linear regression of the fracture length and ground fluid volume, which provides a basis for the absence of microseismic monitoring wells and describes the fracture network. According to the linear regression formula of the single-stage fracture length and the single-stage ground fluid volume in the Chang 6₃ reservoir of the Huaqing area (Figure 11), the regression coefficient is greater than 0.8, which is a strong correlation and can effectively guide the fracture description of highly deviated wells without microseismic monitoring in this area.

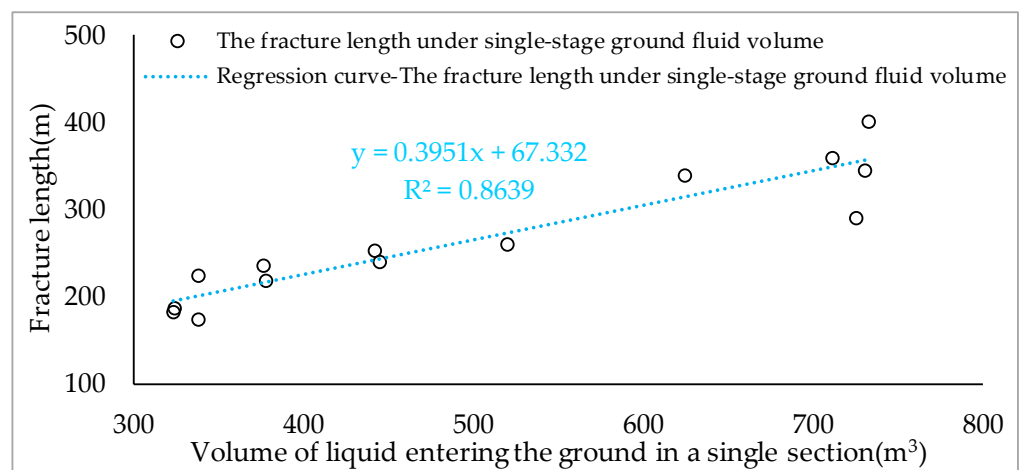


Figure 11. Relationship curve between the single-stage fracturing fracture length and the single-stage ground fluid volume of the Chang 6₃ oil-bearing formation in the Huaqing area.

5. Layered Injection Allocation Calculation Method

5.1. Layered Injection Allocation Calculation Formula

With the above analysis, it can be seen that the effective thickness (h), connectivity coefficient (φ), permeability (k), crude oil viscosity (μ_o), well spacing radius (r_e), wellbore

radius (r_w), production pressure difference (ΔP), and transformation parameters (S) are important factors affecting layered injection allocation. Among them, the crude oil viscosity of the same reservoir is the same, the wellbore radius of the same block is the same, and the production pressure difference between single oil and water wells is the same, which is not used as a calculation parameter. The distance between the oil and water wells ($L = 2r_e$) represents the real displacement distance, which combines the fracturing scale parameters, and the transformation parameters are not used as calculation parameters. The formula of the layered injection ratio (ω) can be obtained:

$$\omega_i = \frac{\varphi_i * k_i * h_i * L_i}{\sum_{i=1}^n \varphi_i * k_i * h_i * L_i} \quad (4)$$

In the formula, $k * h$ represents the stratigraphic coefficient, which reflects the production capacity of the oil and gas layer and the water absorption capacity of the water injection well. The larger the formation coefficient is, the greater the production capacity of the oil and gas layer and the water absorption capacity of the water absorption layers [54]. $k * h * \varphi * L$ is the product of the stratigraphic coefficient, connectivity coefficient, and real displacement distance. It can determine the permeability, water absorption capacity, and water storage capacity of connected sand bodies under the real displacement distance of oil and water wells, which is called the displacement coefficient.

5.2. Calculation Example of Layered Injection Allocation in Highly Deviated Wells

Taking the B193-101 water injection well as the center, four highly deviated wells (B192-101X, B193-100X, B193-102X, and B194-101X) correspond to the surrounding area, and the number of fracturing sections is 6, 6, 5, and 5, respectively. Combined with the regression formula of microseismic monitoring, the fracture length of each highly deviated well is calculated (Figure 12), and the real distance between the oil and water wells in different layers is measured using Geomap 3.6 software (Table 5).

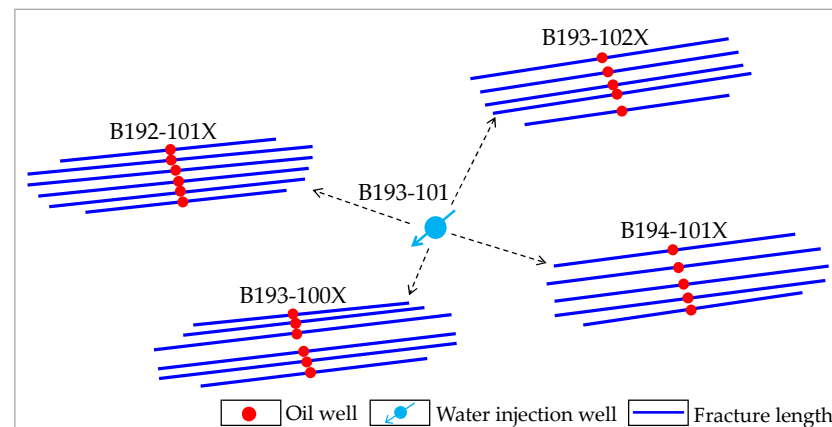


Figure 12. Fracturing network of the well group B193-101.

With the evaluation of the sand body connectivity, the sand body connectivity between highly deviated wells and water injection wells is determined (Figures 13 and 14), the effective sand body thickness is defined, and the displacement coefficient of each perforation point can be obtained. Since highly deviated wells and injection wells are divided into upper and lower sections, the layered injection ratio of different single wells can be obtained by calculating the displacement coefficients of different injection sections. According to the demand of oilfield water injection, the injection allocation of the B193-101 well is set to 20 m^3 , and the injection allocation of each highly deviated well can be calculated using the single well layered injection allocation ratio (Table 5). Through the weighted sum of the injection allocation of the upper and lower sections, the injection allocation of the upper

and lower sections is 13.5 m³ and 6.5 m³, respectively. Because the reasonable injection allocation of the B192-101X well lower section is the minimum injection allocation, which is 5.5 m³, in order to avoid a long-term large amount of water scouring the layer to form a preferential seepage channel, the final reasonable injection allocation of the upper and lower sections is determined to be 14 m³ and 6 m³, respectively.

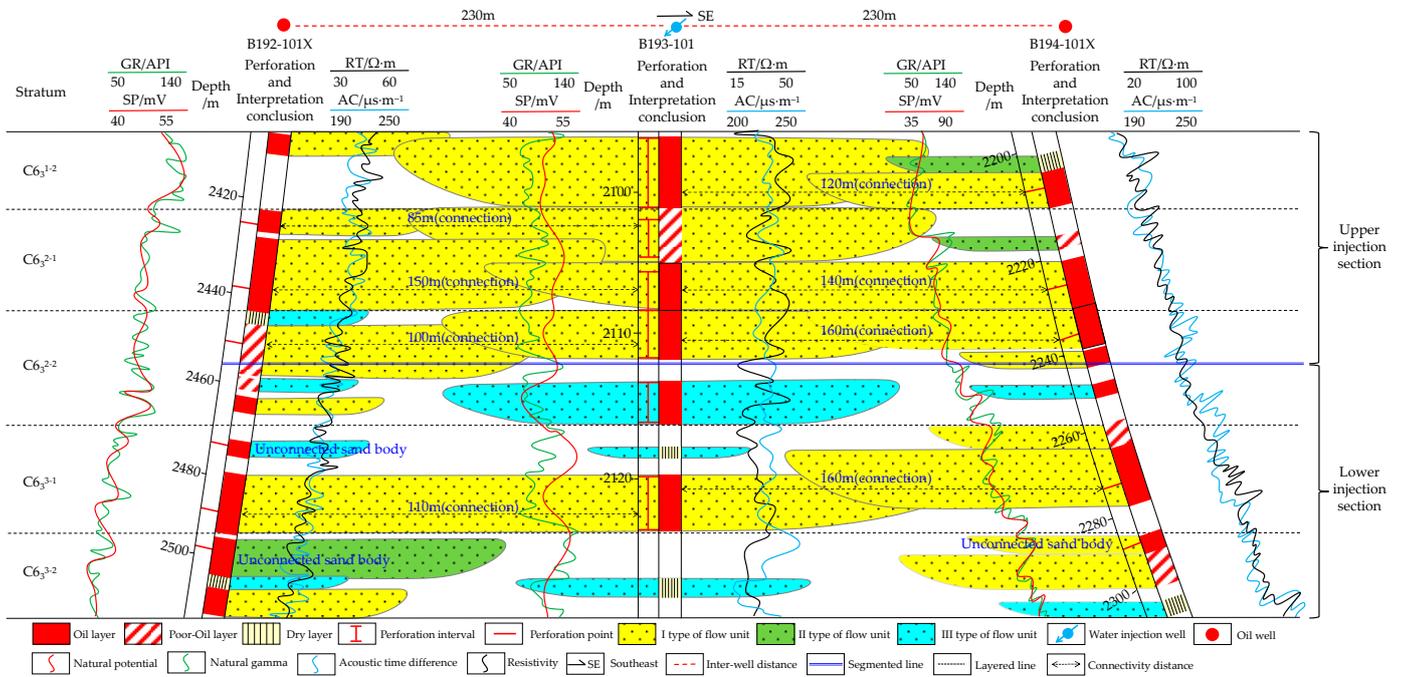


Figure 13. B192-101X well—B193-101 well—B194-101X well sand body connected profile.

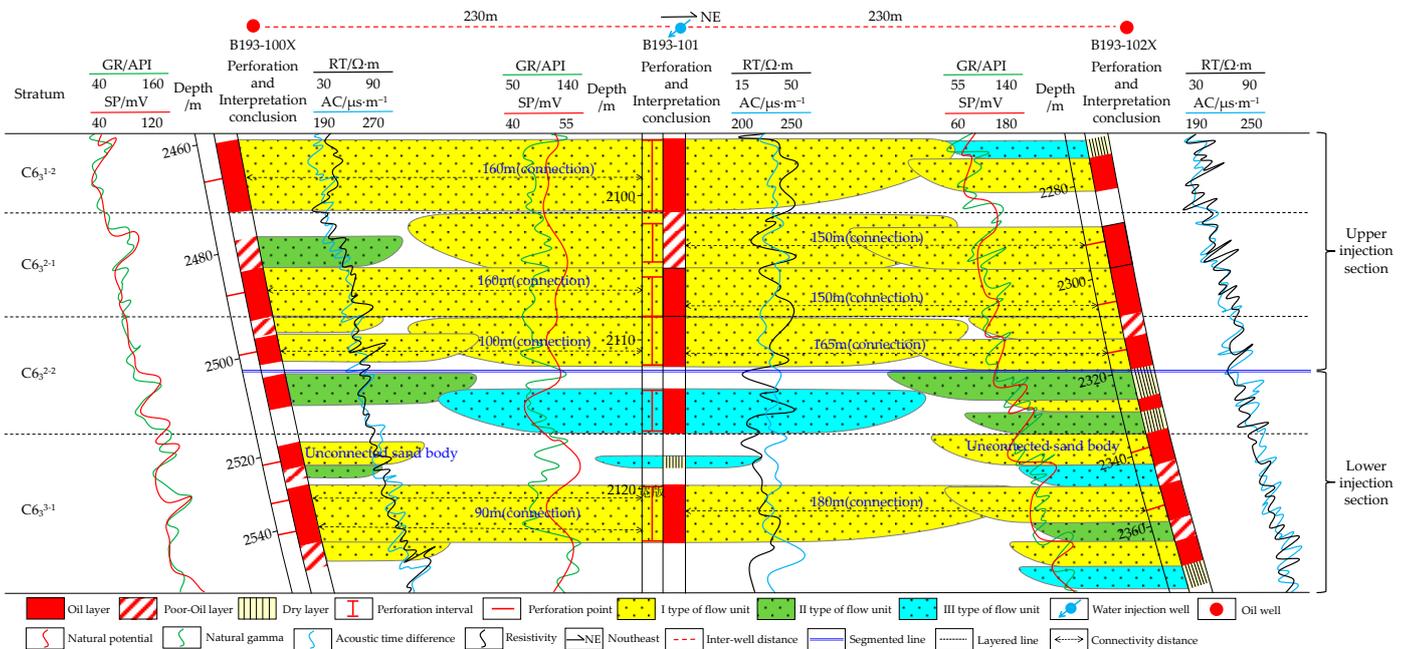


Figure 14. B193-100X well—B193-101 well—B193-102X well sand body connected profile.

Table 5. B193-101 well group of layered injection calculation.

Well Name	Fracturing Section	Real Displacement Distance (m)	Sand Body Connectivity (Yes/No)	Connectivity Degree Coefficient	Permeability (mD)	Effective Thickness (m)	Displacement Coefficient	Water Injection Section	Displacement Coefficient of Water Injection Section	Layered Injection Ratio	Layered Injection Calculation (m ³)
B192-101x	1	85	Yes	0.9	0.23	1.56	27.4	Upper section	199.5	0.72	14.5
	2	150	Yes	0.8	0.23	4.77	131.7				
	3	110	Yes	0.8	0.14	3.28	40.4				
	4	150	No		0.16	0.91	0	Lower section			
	5	110	Yes	1.0	0.2	3.48	76.6				
	6	140	No		0.16	2.98	0				
B194-101x	1	120	Yes	0.8	0.25	2.71	65.0	Upper section	261.8	0.62	12.4
	2	140	Yes	1.0	0.18	5.66	142.6				
	3	160	Yes	0.9	0.33	1.14	54.2				
	4	160	Yes	0.8	0.3	4.17	160.1	Lower section			
	5	190	No		0.24	3.29	0				
B193-100x	1	160	Yes	1.0	0.19	2.15	65.4	Upper section	228.2	0.72	14.4
	2	160	Yes	1.0	0.22	3.71	130.6				
	3	100	Yes	0.8	0.21	1.92	32.3				
	4	110	No		0.24	1.79	0	Lower section			
	5 & 6	90	Yes	1.0	0.22	4.43	87.7				
B193-102x	1	150	Yes	0.8	0.18	2.12	45.8	Upper section	144.4	0.63	12.7
	2	150	Yes	1.0	0.18	1.24	33.5				
	3	165	Yes	0.8	0.21	2.35	65.1				
	4	180	No		0.24	1.68	0	Lower section			
	5	180	Yes	0.9	0.18	2.85	83.1				

6. Production Dynamic Verification of the Layered Water Injection Adjustment Results

Taking B193-101 well group as an example, because the production time of highly deviated wells is different, the production performance of the B193-101 well group was compared and analyzed using the time alignment (Figure 15a). After the B193-101 well group was put into production, it was divided into two sections of layered water injection. The total injection allocation was 30 m³, and the injection allocation of the upper and lower sections was 20 m³ and 10 m³, respectively. In the twelfth month of production, the water cut of the B193-100X well increased rapidly, and then the water cut of the B192-101X and B193-102X wells began to increase gradually. Because of the long-term water injection scouring of a large amount of water, the preferential seepage channel was gradually formed in the high-permeability area of each layer, and the peak water absorption is presented on the water absorption profile (Figure 15b). Therefore, by reducing the water injection volume and applying the method determining the layered injection allocation in highly deviated wells based on connectivity evaluation, the water injection volume was optimized, and the upper and lower sections had water injection volumes of 14 m³ and 6 m³, respectively. In the second, fourth, and fifth months after the injection adjustment, the water cut of the wells B192-101X, B193-100X, and B193-102X began to decrease. In the eighth month after the adjustment of injection allocation for the three highly deviated wells with increased water cut, all the water cuts decreased, and the daily oil production gradually returned to the level before the water cut increased. Among them, B193-100X daily oil production gradually increased, much higher than the level before the water cut increased. From the adjusted injection profile (Figure 15b), it can be seen that the peak water absorption in all water absorbing layers disappeared, achieving uniform displacement. Through production dynamic verification, it can be concluded that the method for determining the layered allocation of highly deviated wells based on connectivity evaluation can effectively guide the layered allocation work of highly deviated wells in the water injection development of oil reservoirs.

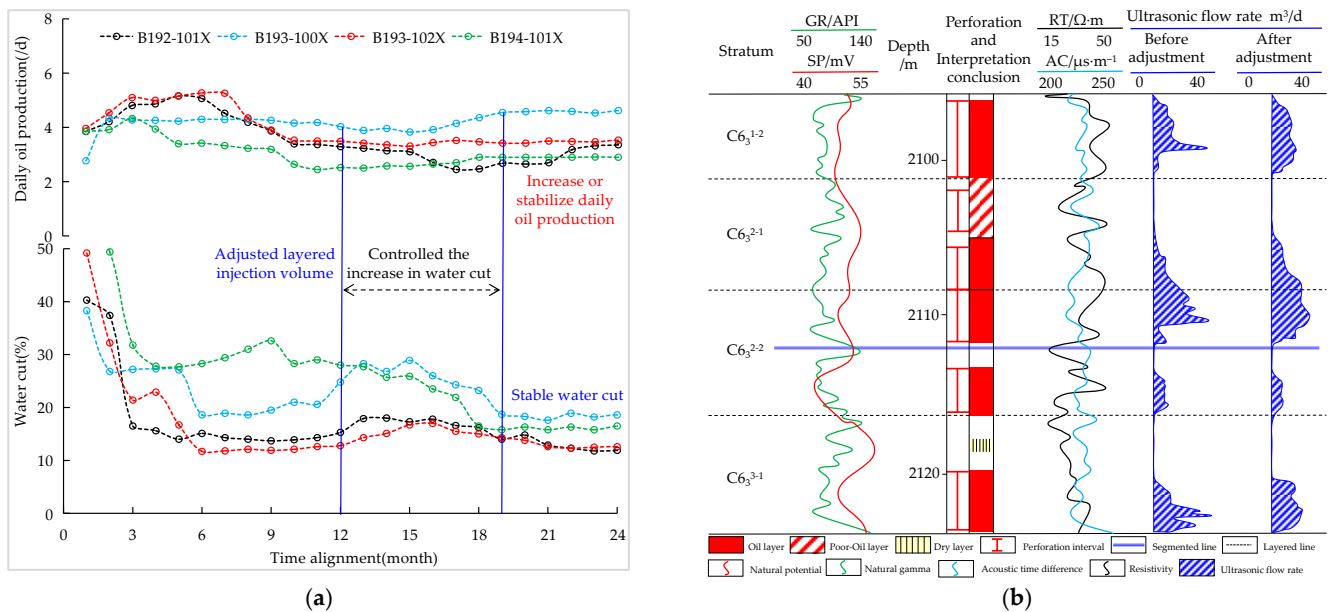


Figure 15. Dynamic verification of layered water injection production. (a) Production curve of the B193-101 well group. (b) Comparison of the water injection profile before and after the injection allocation adjustment in well B193-101.

7. Conclusions

- (1) Four types of vertical stacking patterns and five types of lateral contact relationships of single sand body were identified using sand body configuration. The deposition rate and sediment recharge rate of the turbidite sedimentary system are fast, and the vertical multiperiod channel cutting and stacking type and lateral docking contact of the single sand body are the most developed. Through the combination of three methods of sand body configuration, seepage unit, and single sand body boundary identification, the accuracy of single sand body identification in the target area was 12.6% higher than that of sand body configuration identification.
- (2) The connectivity coefficient characterizes the connectivity ratio of sand bodies, the transition coefficient characterizes the connectivity strength of sand bodies, and the connectivity degree coefficient characterizes the real connectivity of sand bodies. The connectivity degree coefficient can be used as a standard for the quantitative evaluation of single sand body connectivity to determine the connectivity of single sand bodies.
- (3) In order to calculate the reasonable layered injection allocation of water injection reservoirs in highly deviated wells, it is suggested that three to five typical wells under different fracturing scales should be selected for microseismic monitoring, and the correlation between the fracture parameters and the ground fluid volume should be regressed to provide the basis for the lack of microseismic monitoring wells. According to the calculation results of the correlation formula, the fracture network is described, and the real displacement distance of oil and water wells in each layer of highly deviated wells is obtained.
- (4) The new methodology for determination of layered injection allocation in highly deviated wells drilled in low-permeability reservoirs clarifies the connectivity relationship between single sand bodies, describes the method for obtaining the real displacement distance of different layers in highly deviated wells, and determines the reasonable stratified injection allocation between layers. The method's implementation resulted in a 3.6% reduction in the water cut by a year, and a significant increase in the daily oil production of individual wells by 0.5 t/d in the target area. The impact of the injection allocation adjustment was notably significant. This method is scientific and reason-

able, simple and practical, convenient and fast, and has a good application value for the same type of highly deviated wells' water injection development reservoirs.

Author Contributions: Conceptualization, methodology, formal analysis, writing—original draft preparation, M.L.; investigation, data curation, S.J. and L.B.; validation, S.Y.; resources, writing—review and editing, Z.Q. All authors have read and agreed to the published version of the manuscript.

Funding: This research was funded by the National Natural Science Foundation of China (No. 52274007 and No. 51974255), the Scientific Research Program Funded by Shaanxi Provincial Education Department (No. 22JS028 and No. 22JK0597), the Science and Technology Personnel Service Enterprise Project of Xi'an Science and Technology Bureau (No. 22GXFW0148), and the Yan'an University Doctoral Research Initiation Project (No. YAU202303785).

Data Availability Statement: The data presented in this study are available on request from the corresponding author.

Acknowledgments: The authors are grateful for the editors and anonymous reviewers for their constructive comments and suggestions, which greatly improved the quality of the manuscript.

Conflicts of Interest: The authors declare that the research was conducted in the absence of any commercial or financial relationships that could be construed as a potential conflict of interest.

References

1. Qi, Z. *Principles and Design of Oil Production Engineering*; China University of Petroleum Press: Beijing, China, 2000.
2. Hongwen, Y. A discussion using the techniques of production profile determination by the injection profiles of corresponding injection. *Pet. Explor. Dev.* **1990**, *2*, 47–55.
3. Jianchuan, Y. *Study on the Method of Calculation and Optimization of Separated Layer Water Flooding Amount*; Yangtze University: Jingzhou, China, 2015.
4. Dongyi, Z. *The Study of Single WELL injection Allocation Method in Cha Heji Oilfield*; Southwest Petroleum University: Chengdu, China, 2006.
5. Cao, L.; Xiu, J.; Cheng, H.; Wang, H.; Xie, S.; Zhao, H.; Sheng, G. A New Methodology for the Multilayer Tight Oil Reservoir Water Injection Efficiency Evaluation and Real-Time Optimization. *Geofluids* **2020**, *2020*, 8854545. [[CrossRef](#)]
6. Xiaofei, J.; Qizheng, L.; Jing, Y.; Yunpeng, L.; Chunming, Z.; Yanchun, S. A method to allocate injection volume for separate layers in a water-injection well based on the remaining oil distribution. *China Offshore Oil Gas* **2012**, *24*, 38–40.
7. Chuazhi, C.; Hua, J.; Jiehong, D.; Yong, Y.; Jian, W. Reasonable injection rate allocation method of separate-layer water injection wells based on interlayer equilibrium displacement. *Pet. Geol. Recovery Effic.* **2012**, *19*, 94–96. [[CrossRef](#)]
8. Zhaobo, S.; Yunpeng, L.; Xiaofei, J.; Yanlai, L.; Guohao, Z. A method to determine the layered injection allocation rates for water injection wells in high water cut oilfield based on displacement quantitative characterization. *Pet. Drill. Tech.* **2018**, *46*, 87–91. [[CrossRef](#)]
9. Kuiqian, M.; Cunliang, C.; Yingxian, L. Separate-layer water injection allocation based on inter-layer balanced waterflooding. *Spec. Oil Gas Reserv.* **2019**, *26*, 109–112. [[CrossRef](#)]
10. Qinglong, D.; Lihong, Z. A new approach to study layered producing performance of oil and water wells. *Pet. Explor. Dev.* **2004**, *31*, 96–98.
11. Ling, L.; Bingguang, H.; Xingping, T.; Jianli, J.; Yidong, Z. Injection allocation rate determination of well groups using multiple regression method. *Xinjiang Pet. Geol.* **2006**, *27*, 357–358.
12. Xinhua, W.; Jianlin, H.; Ke, A.; Yong, L. Application of BP neural network in well group injection allocation. *Drill. Prod. Technol.* **2006**, 112–113.
13. Zhou, Y.; Lei, S.; Du, X.; Ju, S.; Li, W. Injection-production optimization of carbonate reservoir based on an inter-well connectivity model. *Energy Explor. Exploit.* **2021**, *39*, 1666–1684. [[CrossRef](#)]
14. Mamghaderi, A.; Bastami, A.; Pourafshary, P. Optimization of Waterflooding Performance in a Layered Reservoir Using a Combination of Capacitance-Resistive Model and Genetic Algorithm Method. *J. Energy Resour. Technol.* **2013**, *135*, 013102. [[CrossRef](#)]
15. Zhang, L.; Xu, C.; Zhang, K.; Yao, C.; Yang, Y.; Yao, J. Production optimization for alternated separate-layer water injection in complex fault reservoirs. *J. Pet. Sci. Eng.* **2020**, *193*, 107409. [[CrossRef](#)]
16. Yan, L.; Guangming, L.; Lili, S. Highly-deviated well in exploration and development of Zhangdian oilfield. *Spec. Oil Gas Reserv.* **2003**, 37–39.
17. Yu, Z.; Haiquan, Z.; Yongchen, L.; Chunqiu, G.; Haidong, S. Optimization of development of highly deviated well in gas reservoir with bottom water. *Lithol. Reserv.* **2015**, *27*, 114–118.
18. Smith, R.W.; Colmenares, R.; Rosas, E.; Echeverria, I. Optimized reservoir development with high-angle wells, El Furrial field, Venezuela. *SPE Reserv. Eval. Eng.* **2001**, *4*, 26–35. [[CrossRef](#)]

19. Fair, P.S.; Kikani, J.; White, C.D. Modeling high-angle wells in laminated pay reservoirs. *SPE Reserv. Eval. Eng.* **1999**, *2*, 46–52. [[CrossRef](#)]
20. Abbas, A.K.; Rushdi, S.; Alsaba, M.; Al Dushaishi, M.F. Drilling Rate of Penetration Prediction of High-Angled Wells Using Artificial Neural Networks. *J. Energy Resour. Technol.* **2019**, *141*, 112904. [[CrossRef](#)]
21. Ijasa, O.; Torres-Verdín, C.; Preeg, W.E.; Rasmus, J.; Stockhausen, E. Field examples of the joint petrophysical inversion of resistivity and nuclear measurements acquired in high-angle and horizontal wells. *Geophysics* **2014**, *79*, D145–D159. [[CrossRef](#)]
22. Hu, X.; Fan, Y. Huber inversion for logging-while-drilling resistivity measurements in high-angle and horizontal wells. *Geophysics* **2018**, *83*, D113–D125. [[CrossRef](#)]
23. Puzyrev, V.; Torres-Verdín, C.; Calo, V. Interpretation of deep directional resistivity measurements acquired in high-angle and horizontal wells using 3-D inversion. *Geophys. J. Int.* **2018**, *213*, 1135–1145. [[CrossRef](#)]
24. Wang, L.; Wu, Z.-G.; Fan, Y.-R.; Huo, L.-Z. Fast anisotropic resistivities inversion of logging-while-drilling resistivity measurements in high-angle and horizontal wells. *Appl. Geophys.* **2021**, *17*, 390–400. [[CrossRef](#)]
25. Duan, M.; Miska, S.; Yu, M.; Takach, N.; Ahmed, R.; Zettner, C. Critical Conditions for Effective Sand-Sized Solids Transport in Horizontal and High-Angle Wells. *SPE Drill. Complet.* **2009**, *24*, 229–238. [[CrossRef](#)]
26. Wang, Y.; Zhou, C.; Yi, X.; Li, L.; Chen, W.; Han, X. Technology and Application of Segmented Temporary Plugging Acid Fracturing in Highly Deviated Wells in Ultradeep Carbonate Reservoirs in Southwest China. *ACS Omega* **2020**, *5*, 25009–25015. [[CrossRef](#)] [[PubMed](#)]
27. Meng, F.; He, D.; Yan, H.; Zhao, H.; Zhang, H.; Li, C. Production performance analysis for slanted well in multilayer commingled carbonate gas reservoir. *J. Pet. Sci. Eng.* **2021**, *204*, 108769. [[CrossRef](#)]
28. Waburoko, J.; Xie, C.; Ling, K. Effect of Well Orientation on Oil Recovery from Waterflooding in Shallow Green Reservoirs: A Case Study from Central Africa. *Energies* **2021**, *14*, 1223. [[CrossRef](#)]
29. Wang, H.; Xue, S.; Gao, C.; Tong, X. Inflow performance for highly deviated wells in anisotropic reservoirs. *Pet. Explor. Dev.* **2012**, *39*, 239–244. [[CrossRef](#)]
30. Wang, K.; Wang, L.; Adenutsi, C.D.; Li, Z.; Yang, S.; Zhang, L.; Wang, L. Analysis of Gas Flow Behavior for Highly Deviated Wells in Naturally Fractured-Vuggy Carbonate Gas Reservoirs. *Math. Probl. Eng.* **2019**, *2019*, 6919176. [[CrossRef](#)]
31. Zhang, Q.; Zhang, L.; Liu, Q.; Jiang, Y. Pressure Performance of Highly Deviated Well in Low Permeability Carbonate Gas Reservoir Using a Composite Model. *Energies* **2020**, *13*, 5952. [[CrossRef](#)]
32. Wang, L.; Lv, D.; Hower, J.C.; Zhang, Z.; Raji, M.; Tang, J.; Liu, Y.; Gao, J. Geochemical characteristics and paleoclimate implication of Middle Jurassic coal in the Ordos Basin, China. *Ore Geol. Rev.* **2022**, *144*, 104848. [[CrossRef](#)]
33. Cui, J.; Li, S.; Mao, Z. Oil-bearing heterogeneity and threshold of tight sandstone reservoirs: A case study on Triassic Chang7 member, Ordos Basin. *Mar. Pet. Geol.* **2019**, *104*, 180–189. [[CrossRef](#)]
34. Ding, F.; Shi, C.Q.; Zhang, P.H. Characteristics of the Braided River Deposits in the Tenth Member of Jurassic Yan'an Formation From Jiyuan Area in the Western Ordos Basin, China. *Pet. Sci. Technol.* **2013**, *31*, 2422–2430. [[CrossRef](#)]
35. Tian, Y.; Yingchang, C.; Jingchun, T.; Xiaobing, N.; Shixiang, L.; Xinping, Z.; Jiehua, J.; Yian, Z. Deposition of deep-water gravity-flow hybrid event beds in lacustrine basins and their sedimentological significance. *Acta Geol. Sin.* **2021**, *95*, 3842–3857. [[CrossRef](#)]
36. Xinping, Z.; Qing, H.; Jiangyan, L.; Shixiang, L.; Tian, Y. Features and origin of deep-water debris flow deposits in the Triassic Chang 7 Member, Ordos Basin. *Oil Gas Geol.* **2021**, *42*, 1063–1077. [[CrossRef](#)]
37. Fudol, Y.A.; Zhao, Y.; Liu, H.; Zhou, S.; Li, Y.; Li, X. Origin and reservoir properties of deep-water gravity flow sediments in the Upper Triassic Ch6–Ch7 members of the Yanchang Formation in the Jinghe Oilfield, the Southern Ordos Basin, China. *Energy Explor. Exploit.* **2019**, *37*, 1227–1252. [[CrossRef](#)]
38. Larue, D.K.; Hovadik, J. Connectivity of channelized reservoirs: A modelling approach. *Pet. Geosci.* **2006**, *12*, 291–308. [[CrossRef](#)]
39. Lv, A.; Li, X.; Yu, M.; Li, G.; Wang, S.; Peng, R.; Zheng, Y. The method of the spatial locating of macroscopic throats based-on the inversion of dynamic interwell connectivity. *Open Phys.* **2017**, *15*, 313–322. [[CrossRef](#)]
40. Gong, M.; Zhang, J.; Yan, Z.; Wang, J. Prediction of interwell connectivity and interference degree between production wells in a tight gas reservoir. *J. Pet. Explor. Prod. Technol.* **2021**, *11*, 3301–3310. [[CrossRef](#)]
41. Yin, X.; Huang, W.; Lu, S.; Wang, P.; Wang, W.; Xia, L.; Yao, T. The connectivity of reservoir sand bodies in the Liaoxi sag, Bohai Bay basin: Insights from three-dimensional stratigraphic forward modeling. *Mar. Pet. Geol.* **2016**, *77*, 1081–1094. [[CrossRef](#)]
42. Donselaar, M.E.; Overeem, I. Connectivity of fluvial point-bar deposits: An example from the Miocene Huesca fluvial fan, Ebro Basin, Spain. *AAPG Bull.* **2008**, *92*, 1109–1129. [[CrossRef](#)]
43. Zhang, L.; Wang, H.; Li, Y.; Pan, M. Quantitative characterization of sandstone amalgamation and its impact on reservoir connectivity. *Pet. Explor. Dev.* **2017**, *44*, 226–233. [[CrossRef](#)]
44. Yu, Z.; Yang, J.; Song, X.; Qiao, J. Fine Depiction of the Single Sand Body and Connectivity Unit of a Deltaic Front Underwater Distributary Channel: Taking the Third Member of the Dongying Formation in the Cha71 Fault Block of the Chaheji Oilfield as an Example. *Geofluids* **2021**, *2021*, 1401051. [[CrossRef](#)]
45. Guangyi, H.; Tinggen, F.; Fei, C.; Yongquan, J.; Laiming, S.; Xu, L.; Dakun, X. Theory of composite sand body architecture and its application to oilfield development. *Oil Gas Geol.* **2018**, *39*, 1–10. [[CrossRef](#)]

46. Liu, R.; Sun, Y.; Wang, X.; Yan, B.; Yu, L.; Li, Z. Production Capacity Variations of Horizontal Wells in Tight Reservoirs Controlled by the Structural Characteristics of Composite Sand Bodies: Fuyu Formation in the Qian'an Area of the Songliao Basin as an Example. *Processes* **2023**, *11*, 1824. [[CrossRef](#)]
47. Shi, T.; He, S.; Yuan, K.; Liu, M.; Wang, M.; Tu, X.; Chang, L. Analysis of Oil-Water Distribution Law and Main Controlling Factors of Meandering River Facies Reservoir Based on the Single Sand Body: A Case Study from the Yan 932 Layer of Y Oil Area in Dingbian, Ordos Basin. *Geofluids* **2023**, *2023*, 4273208. [[CrossRef](#)]
48. Hearn, C.L.; Ebanks, W.J., Jr.; Tye, R.S.; Ranganathan, V. Geological factors influencing reservoir performance of the Hartzog Draw field, Wyoming. *J. Pet. Technol.* **1984**, *36*, 1335–1344. [[CrossRef](#)]
49. Huanqing, C.; Yongle, H.; Lin, Y.; Min, T. Advances in the study of reservoir flow unit. *Acta Geosci. Sin.* **2010**, *31*, 875–884.
50. Yang, Z.; Wang, S.; Chen, J.; Jing, S. Architecture, genesis, and the sedimentary evolution model of a single sand body in tight sandstone reservoirs: A case from the Permian Shan-1–He 8 members in the northwest Ordos Basin, China. *Front. Earth Sci.* **2023**, *10*, 1003818. [[CrossRef](#)]
51. Ebanks, W.J., Jr. Flow unit concept-integrated approach to reservoir description for engineering projects. *Am. Assoc. Pet. Geol. Bull.* **1987**, *71*, 551–552.
52. Shedid, S.A. A new technique for identification of flow units of shaly sandstone reservoirs. *J. Pet. Explor. Prod. Technol.* **2017**, *8*, 495–504. [[CrossRef](#)]
53. Jie, A.; Meirong, T.; Zongxiong, C.; Wenxiong, W.; Wenbin, C.; Shunlin, W. Transformation of development model of horizontal wells in ultra-low permeability and low-pressure reservoirs. *Lithol. Reserv.* **2019**, *35*, 134–140. [[CrossRef](#)]
54. Hanqiao, J.; Jun, Y.; Ruizhong, J. *Principles and Methods of Reservoir Engineering*; China University of Petroleum Press: Beijing, China, 2006.

Disclaimer/Publisher's Note: The statements, opinions and data contained in all publications are solely those of the individual author(s) and contributor(s) and not of MDPI and/or the editor(s). MDPI and/or the editor(s) disclaim responsibility for any injury to people or property resulting from any ideas, methods, instructions or products referred to in the content.